Received: 16 June 2020 | Revised: 19 February 2021 | Accepted: 19 March 2021

DOI: 10.1002/suco.202000351

TECHNICAL PAPER

fib CEB-FIP WILEY

Bond and re-anchoring tests of post-tensioned steel tendon in case of strand failure inside cement grouting with voids

Olli Asp | **Joonas Tulonen** | **Lauri Kuusisto** | **Anssi Laaksonen**

Tampere University, Faculty of Built Environment, Tampere, Finland

Correspondence
Olli Asp, Tampere University, Faculty of Built Environment, Tampere, Finland.
Email: olli.asp@tuni.fi

Abstract

Grouted tendons are commonly used in construction of bridges and other post-tensioned structures. The quality of grouting is essential to provide the durability and robustness of the structure. In this paper, the bond and re-anchoring of post-tensioned tendons in grout in case of tendon failure is assessed. A set of tests were conducted to simulate the failure of a post-tensioned tendon in the beam. The results were compared with the theory of prestressing strand anchoring in concrete. In the tests, the re-anchoring and bond lengths were measured in case of complete grout and incomplete grout with void. In the case of incomplete grout, the increase in re-anchoring length is observed. In the case of overlapping re-anchoring and bond length, the bond length and tendon slip increase significantly. A limited re-anchoring length of tendon in incomplete grout increases the robustness of the structure, as the broken tendon can maintain its effectiveness outside of the failure region. The existing calculation model shows a good match with test results, and therefore it is suitable for the analysis of structures with broken tendons.

KEYWORDS

bond, grouting, post-tensioned, re-anchor, tendon

1 | INTRODUCTION

A common way of constructing a post-tensioned concrete bridge in Finland is to place metal ducts inside a formwork of a bridge girder or a slab in which the prestressing steel is installed after the concrete superstructure is cast. Also, non-metallic ducts are used for example, in Central Europe, but they are not common in Finland and thus not discussed in this paper. A tendon consisting of many prestressing steel strands is then tensioned to the desired force and the metal ducts are injected with cement-based grout, which should provide the prestressing steel with essential protection from harmful substances and thus prevent damage in the steel. If the quality of grouting is good and the structure is designed and manufactured so that water ingress in the concrete at the proximity of prestressing steel is low, the probability of prestressing steel corrosion should be low. One drawback in this method is that sufficient quality of grouting can be very hard to determine on-site and possible corrosion problems during the service life of a bridge are hidden deep inside the

Discussion on this paper must be submitted within two months of the print publication. The discussion will then be published in print, along with the authors' closure, if any, approximately nine months after the print publication.

concrete structure. Corrosion failures of prestressing tendons and strands have been observed in many cases around the world and can lead to failure or collapse of complete bridge structures. In the UK, the construction of grouted and post-tensioned bridges was even banned in 1992 by the Department of Transport until the grouting standards could be reviewed in response to observed defects in grouting.[1]

The effects of strand corrosion and grout voids on the bending behavior of a beam have been studied by Wang et al.[2,3] with load tests on beams that had undergone electrochemically accelerated corrosion. The study showed that the strand corrosion and grouting defects have a large influence on the ultimate strength and cracking behavior of beams with a single post-tensioned strand.

If a prestressing tendon would fail completely inside the concrete structure, the effects of the failure on the structure depend largely on the bond characteristics between the tendon and the concrete. If the tendon is unbonded, then the prestressing effects of that tendon would disappear along the complete length of a prestressed member, since the prestressing steel would return to its unloaded length after rupture. If the bond strength and stiffness are infinite, the prestressing effects would only diminish in the exact cross section where the tendon failure occurred. The reality is somewhere in between these extreme cases.

Tendons in post-tensioned bridges consist of many strands in a single duct, and the required bond is formed between strands, grout, duct and concrete and is therefore a far more complex matter since a single strand may be in contact with another strand, grout and duct at the same time. It is also likely that in an area where there is a high risk of prestressing steel corrosion, multiple strands are affected and the local rupture of a whole tendon is possible, as was demonstrated in several externally post-tensioned bridges in the USA at the beginning of the millennium.[4]

The transfer and transmission length of single strands in concrete have been researched quite extensively,[5,6] since the phenomenon is essential for prefabricated and prestressed concrete elements, as can be seen in an overview on the subject by Martí-Vargas et al. in their paper[7] about an experimental programme to determine transmission and anchorage length in relation to concrete properties. Design equations for single-strand transfer design in concrete can be found in most design standards, for example in Eurocodes.[8] The bond behavior of multistrand tendons cast in grout without prestress has been studied by Wang et al. in.[9] To assess the realistic behavior of post-tensioned and grouted tendons, the stress change in strands needs to be considered.

In this study, the aim is to assess the effects of the grout defects on the bonding and re-anchoring characteristics of grouted multistrand tendons. Concrete test specimens with a 0.4 m × 0.4 m cross section were manufactured in two sets. The first set has a length of 3 m to make sure that the complete re-anchoring length of all strands could be observed and to also study the transmission length of a complete strand bundle separately. The second set has lengths of 1.7 m and 1.2 m to study the overlapping phenomenon of re-anchoring and transmission lengths in an insufficiently grouted and fully grouted specimen, respectively. To study a re-anchoring length of multistrand tendons in both sufficiently and insufficiently grouted ducts, 16 concrete test specimens with 85-mm ducts and 12 0.62″ seven-wire post-tensioned strands each were manufactured, and their behavior in cases of strand releasing and additional stressing was observed with tightly spaced strain gauges attached to the concrete surface.

2 | EXPERIMENTAL TEST

2.1 | Test setup

The test setup shown in Figures 1 and 2 is built to assess a bond and re-anchoring characteristics between tendon strands and cement grout in case of complete grouting, which fills the tendon duct and in case of incomplete grouting with void in the grout. The test setup consists of a reinforced concrete beam, two prestressing chairs, prestressing strands, a hydraulic jack and necessary wedges, and wedge plates to anchor the strands in the post-tensioning process. The prestressing chairs are made of two U-profile steel beams which are joined in the ends by thick steel plates which have a hole in the center for the prestressing strands to pass through. The construction of prestressing chairs in each end of the beam is a bit different. In the passive end, the strands can be released to simulate the breakage of strands by using a special release mechanism for strand anchors. In the active end, the additional tension is provided by pulling on strands with a hydraulic jack. Strain gauges are glued (beams #1–6: 7 pcs, and beams #7–16: 9 pcs) along the centerline of the side surface of the beam to measure a change in the strain of concrete. The strain gauges are also attached onto the sides of the prestressing chairs to measure the force acting on the ends of the chairs and beam. The force-strain relations of the chairs are calibrated by using a compressive hydraulic press with calibrated force transducer.

In the test, concrete specimen beams are cast with tendon duct inside. Prestressing anchoring/release devices, later chairs, are placed on both ends of the beam after the curing of the concrete. The strands are placed inside the duct and through the prestressing chairs, and

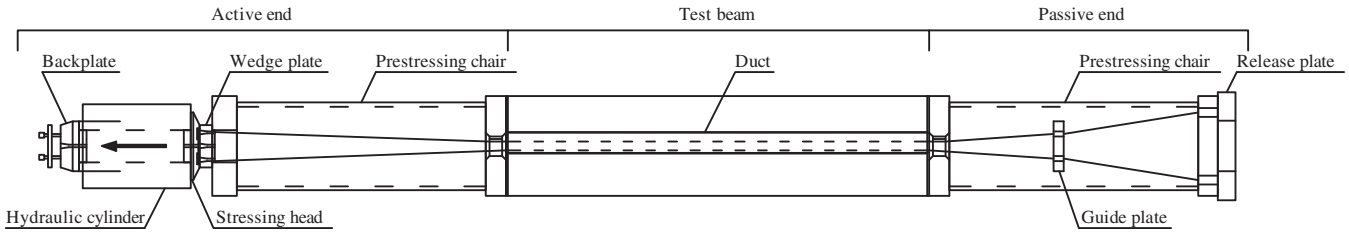

FIGURE 1 Schematic drawing of test setup

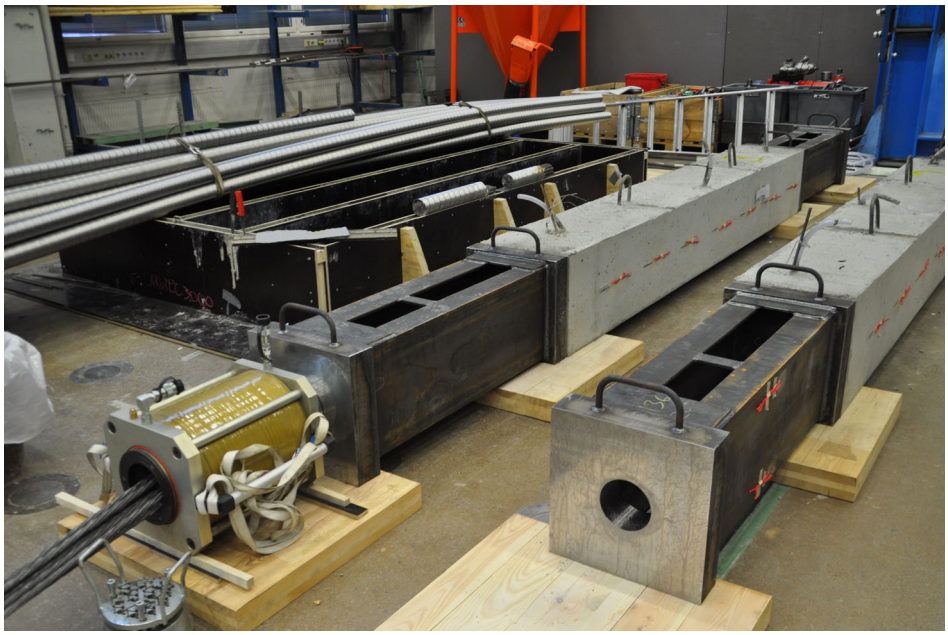

FIGURE 2 Test beams with hollow cylinder jack assembled on active end of the beam

the complete assembly consisting of the beam and two prestressing chairs is prestressed by pulling the strands against the prestressing chairs with a hydraulic jack. The target level of the post-tensioning force after locking the strands in the active end of the wedge plate is 1800 kN, which corresponds to a strand stress of 1000 MPa with 12 strands. After prestressing, the duct is grouted with cement grout. In beams 2 and 3, which were tested first, the prestressing of bottom four strands was limited to approximately 500 MPa since there was concern of premature beam failure under high stresses. In all subsequent tests, all of the strands were stressed to the same level of 1000 MPa.

After the curing of the grout, the tendons are released as pairs from the passive end and the change in strain of concrete is measured with the strain gauges along the length of the beam (shown in Figure 3). The strands are released in sets of four strands. After the release of a set of four strands, additional stressing of 100 MPa at each step is applied on strands in the active end of the beam to simulate the stress increase in the tendon in the ultimate limit state when the concrete has cracked. When all of the strands are released from the passive end, the ultimate stress is applied to strands on the active end to test the bonding of strands. The force in a hydraulic jack is limited to 2.7 MN, which means a stress level of 1500 MPa in the strands in case the bond between the strands and the grout does not fail.

2.2 | Test specimens

The test specimens are 400 mm × 400 mm concrete beams with steel tendon duct placed inside. The tendon duct is positioned eccentrically to achieve a centric compressive force on the beam as the tendons are lying on the bottom of the duct. Eccentricity is introduced to create similar conditions for the strands as they would have if the tendon would be in a curved duct in a real bridge structure. The center of gravity of the tendon strands and the center of gravity of the concrete beam should match. The length of the beams vary from 1230 mm to 3000 mm as shown in Table 1.

The concrete used in beams is C50/60 concrete with reinforcement to prevent cracking due to possible concentrated forces caused by prestressing and the release of tendons. The tendon duct is corrugated steel duct

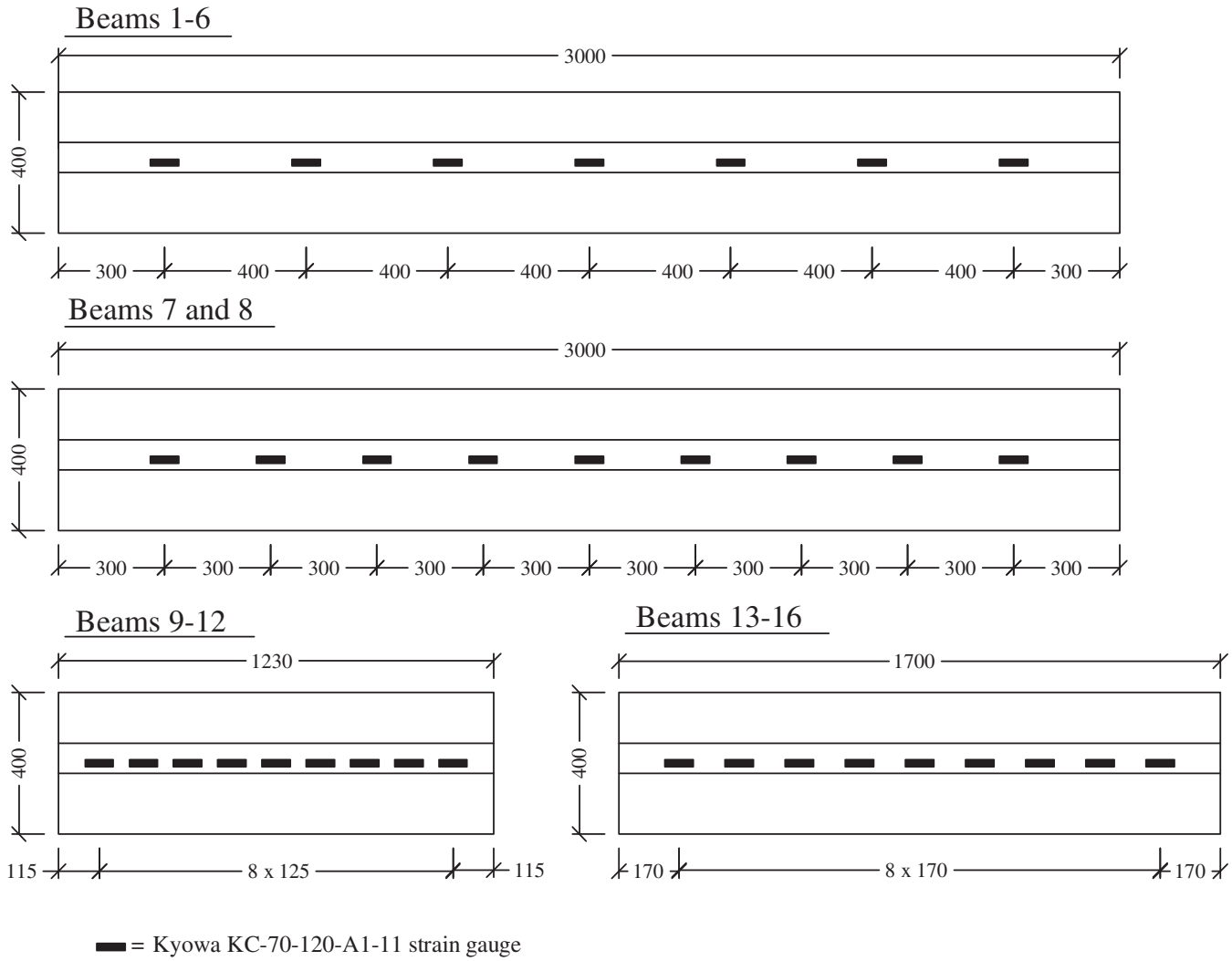

FIGURE 3 Strain gauge locations in the test beams

Set #	Beam #	Length [mm]	Grouting	Reference	Notes
I	1...4	3000 mm	Complete (C)	I-Beam#-3000-C	
II	5...8	3000 mm	Incomplete (IC)	II-Beam#-3000-IC	
III	9...12	1230 mm	Complete (C)	III-Beam#-1230-C	
IV	13...16	1700 mm	Incomplete (IC)	IV-Beam#-1700-IC	

TABLE 1 The naming and characteristics of the beams in test

according to standard EN 523:2003.[10] The duct is identical with the one used commonly in the construction of post-tensioned bridges. The prestressing steel is 0.62″ 7-wire-strand, St 1600/1860 with a 15.7-mm nominal diameter. The cross-sectional area of a single strand is 150 mm^2. The number of strands in each beam is 12, and the total area of prestressing steel is 1800 mm^2.

The void for incompletely grouted tendon ducts in beam sets II and IV is achieved by placing a cut polystyrene filling inside the duct to prevent the grout from filling the duct completely. The height of the polystyrene obstacle is 20 millimeters.

The strain of concrete is measured using Kyowa KC-70-120-A1-11L1M2R strain gauges. The strain of the prestressing chairs, and therefore the prestressing force, is measured with four Kyowa KFGS-5-120-C1-11L1M2R strain gauges per prestressing chair. The pull-out of tendons is measured using a Novotechnik TS-100 transducer gauge. The data is collected using a data logger and a computer.

2.3 | Test procedure

At the beginning of the test, the concrete beam is prestressed and the grout in the tendon duct is cured. The test consists of the following release stages:

- 1st release*, four uppermost strands
  - additional stress** of 100 MPa
- 2nd release*, four middle strands
  - additional stress** of 100 MPa
- 3rd release*, last four strands, all strands released
  - additional stress** of 100 MPa
- Additional stressing to 2.7 MN, the maximum force of the hydraulic jack
- Removing the hydraulic jack and releasing the anchored tendons by cutting them inside the prestressing chair at the active end

  * from passive end.

  **from active end with duration of 3 min.

The sequence of the releasing of strands is simulating the corrosion damage progressing from the uppermost strands near the void to the lower ones. The additional stressing simulates the effect of stress increase in the tendon due to live loads during the deterioration process.

The tendons are released from the stressing chair at the passive end and additional stressing force is applied on the active end with a hydraulic jack by pulling tendons against the chair at the active end. The additional stressing forces are held for 3 min. Additional stressing towards the maximum force of the hydraulic jack is applied in steps of 250 kN, holding the load for 3 min before next step.

In Figure 4(a) the schematic figure of the measured chair force during the test is presented at each end of the beam. The additional stressing in the active end (dashed line, F_{active}) varies between F_0 and F_A. In case of permanent deformation or slip between tendon and grout, the drop ΔF_A in the force in the active end could be observed. In this case, the force in the active end does not return to the original level (dotted line) in Figure 4(a). In Figure 4(b) the schematic figure of force in tendon during the test is presented, F_{PO} the pull-out force at active end and F_{REA} the re-anchored force in passive end.

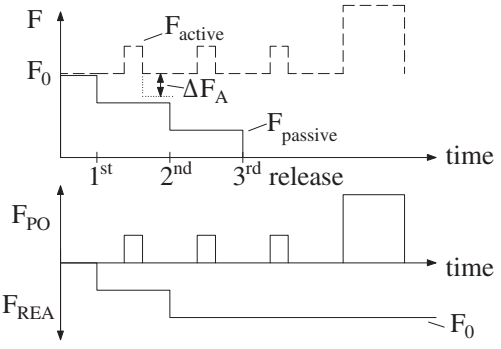

FIGURE 4 (a) Force-time history on active and passive end of test specimen (b) pull-out force and released force during the test

3 | CALCULATION THEORY

In practice, the design related to the bond of pretensioned strands is solved using a simplified bond stress distribution assuming linear transmission of force between tendon and concrete. For a better understanding of the influence of various parameters on transmission length and anchorage capacity, a more precise model of the bond stress distribution is required.

3.1 | Bond stress versus slip

According to the FIB Bond of reinforcement in concrete,[11] the slip distribution along an embedded strand can be described by a second order differential equation considering equilibrium and compatibility and assuming elastic material behavior and a bond stress that only depends on the slip. Based on this equation, an analytical solution can be derived in order to describe the bond stress-slip relation:

$$\tau_b = \eta_1 \eta_2 f_{ci}^{0,5} \left(\frac{\delta}{\theta_p} \right)^{\eta_3}, \quad (1)$$

where

τ_b is bond stress,

δ is slip, between strand and concrete,

θ_p is the nominal diameter of the strand,

f_{ci} is the compressive strength of concrete,

$\eta_1 = 1.35$; 1.0 and 0.65 for the upper bound, mean and lower bound of the bond stress,

η_2 and $\eta_3$are experimental constants based on the diameter of the strand,

$\eta_2 = 2.055$ and $\eta_3 = 0.25$, when $\theta_p = 12.8$ mm.

In the Equation 1, the bond stress τ_b is considered to be proportional to the square root of the concrete compressive strength at transfer. In the case of this experiment the compressive strength of the grout is used in calculations. The grout prisms are cast during the injection of beams. The compressive strength of the grout is tested according to SFS-EN 445[12] on the same day as the re-anchoring and pull-out tests of the test beams. The average compressive strength of grout on a test day is 33.5 MPa with 2.9 MPa standard deviation.

3.2 | Bond stress versus slip and steel stress change

An invariable bond stress-slip relation does not take into account the influence of transverse deformation of the strand due to the Poisson effect on bond stress. However, pull-out and push-in tests (Den Ujil, 1992)[5] have concluded that the bond resistance is clearly influenced by the Poisson effect. This resulted in the following equation:

$$\tau_b = 3 + 0{,}4\delta - 2.5 * 10^{-3}\Delta\sigma_p + 1.5 * 10^{-3}\left|\Delta\sigma_p\right|, \quad (2)$$

where

τ_b is bond stress [MPa]

δ is slip between strand and grout [mm]

$\Delta\sigma_p$ is change of steel stress [MPa]

The terms on the right side of the equation are related to adhesion, lack-of-fit effect, Poisson effect and pitch effect, respectively. It is notable that the relative deformation associated with adhesion has been neglected.

3.3 | Characteristics of multistrand tendon

Equations (1) and (2) give the bond stress in relation to bond area in MPa. This requires determining the bond perimeter of the strand bundle. A bond perimeter of a single strand is determined by assuming the effective bond to be present only on the outer surface of wire with direct contact to grout, while the internal space between wires in a strand is neglected. In a strand bundle, it is assumed that only the outer strands transmit prestressing force and that the effective transmission occurs in approximately half of their sphere.

This resulted in an approximate bond sphere of a strand bundle of:

$$d_{wire} = 2 * \sqrt{\frac{A_{sp}}{7\pi}} = 5.2\,mm, \quad (3)$$

$$p = 6 * \frac{240}{360}\pi * d_{wire} = 65.6\,mm, \quad (4)$$

$$p_{tot} = n_{p.out} * 0.5 * p = 328.0\,mm, \quad (5)$$

where$A_{sp}$is the cross-sectional area of a single strand,

d_{wire} is the diameter of a single wire of a strand,

p is the bond perimeter of a single strand

p_{tot} is the bond perimeter of a strand bundle

$n_{p.out}$is the number of strands on outer perimeter of bundle

The principle of determining the bond perimeter of a single strand and strand bundle is shown in Figure 5. The perimeter for bonding has a significant effect on force transmission between strands and grout. Therefore, in the case of incomplete grout it is assumed that the bond area should be reduced to covering only those strands with assumed sufficient grout with an adequate confining effect. In Figure 5, the bond perimeter in complete grout with no grouting defect (void) is presented with a red line, and the assumed bonding perimeter in the case of incomplete grout with a red line and dark gray filling.

The actual cracking behavior of grout, observed from sawn cross sections of test beam 5 presented in Figure 6 seems to match well with the model. The cracking of grout towards the (polystyrene)void can be seen in Figure 6.

3.4 | A numeric procedure

The distribution of tendon force along the re-anchoring length can be calculated using a numerical method.

$$\varepsilon_i = \frac{F_i}{A_{sp.tot}E}, \quad (6)$$

$$\delta_i = \delta_{i-1} + (\varepsilon_0 - \varepsilon_i) * \varsigma, \quad (7)$$

$$\Delta\sigma_i = \frac{F_i - F_0}{A_{sp}}, \quad (8)$$

In which,F_iForce in tendon on cross section i,

F_0 Force in tendon on cross section 0 (x = 0 mm)

ε_i Tendon strain on cross section i,

$A_{sp.\ tot}$ Tendon area (total area of strands),

E Young's modulus of prestressing steel 195 GPa

δ_i relative slip of tendon on cross section i

$\Delta\sigma_i$ change in tendon stress on cross section i.

ς Calculation step ($\varsigma = 0.1\ mm$).

The bond stress τ_n versus slip is calculated according to Equation (1), and the bond stress versus slip and steel stress change according to Equation 2. The tendon force in the next cross section is calculated according to the equation:

$$F_{i+1} = F_i - \tau_i * p_{tot} * \varsigma, \quad (9)$$

In which,$\tau_i$bond stress on cross section i

p_{tot} bond perimeter of strand bundle according to Equation 5

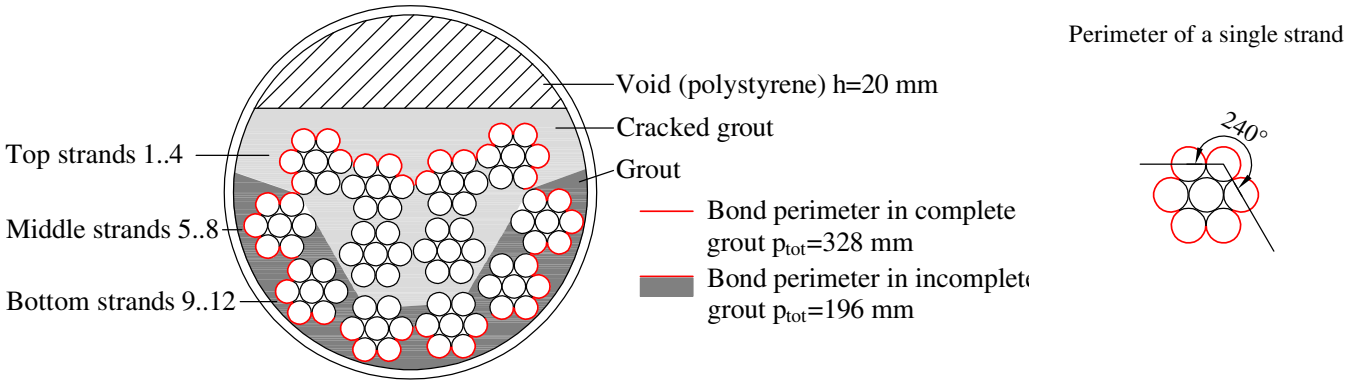

FIGURE 5 Strand layout in tendon duct, arrangements for void in test and effective perimeters for tendon

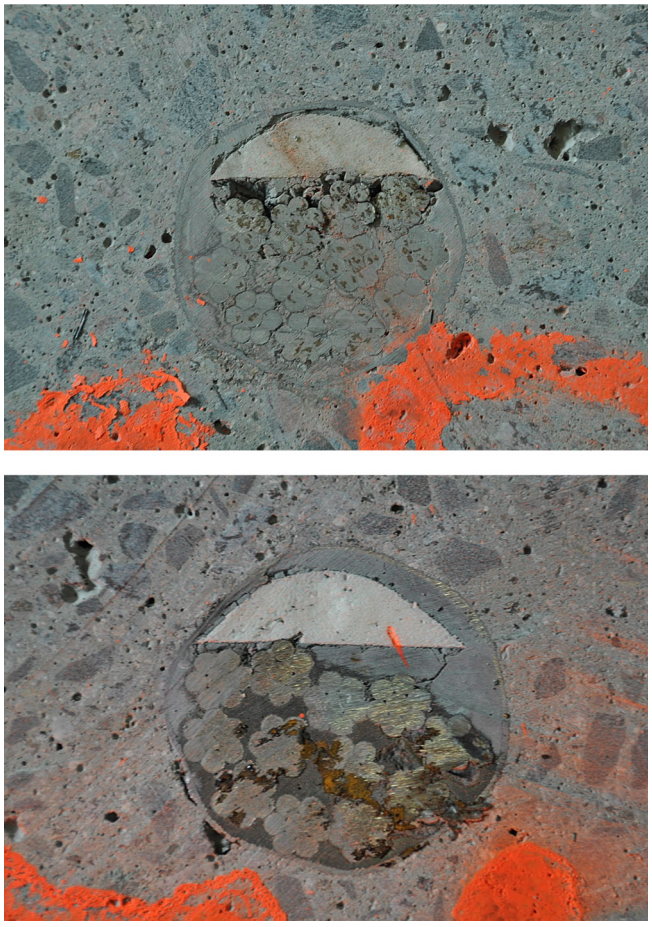

FIGURE 6 Sawn cross sections of test beam 5. In the middle of the beam (left), 300 mm from the end of the beam (right)

The calculation procedure for the re-anchoring length of the released strand bundle is presented in Figure 7. The calculation is started at an arbitrary cross section with boundary conditions $F_0 = F_{00}$ and $\delta_0 = 0$. The location of the cross section is still unknown. The calculation progresses step by step until condition $F_{i+1} < 0$ kN is met, meaning that the initial prestressing force is completely transferred to the surrounding grout and the i^{th} cross section is the cross section with zero tension in the strand, i.e. the end of the beam (breaking point of the tendon).

4 | RESULTS

4.1 | The analysis of the test results

Change of the axial force along the beam length will be used to measure the re-anchoring and bond lengths of the tendons. Measurement of the axial force is done by strain gauges on the surface of the beam side. Two main factors affect the measurements: shear lag and heterogenous properties of the concrete. Shear lag is related to the distance of the tendons to the strain gauge since the local change in axial stress of concrete in the middle of one cross-section does not directly translate to a change of axial stress in the same cross-section at the surface. Shear lag phenomenon is not studied here and its effect is reduced by attempt to keep the tendon-to-surface distance small enough while keeping the concrete cross-section area reasonable. It can be estimated that the measured results could be shifted 0.1–0.15 meters towards the beam end due to shear lag, but it is not considered in the results.

The heterogenous properties of the concrete cause some variance in the strain readings on the concrete surface and the readings between different gauges cannot be directly compared as they would indicate a change in the beam axial force distribution when there actually is none. Therefore, calibration of the strain gauges for each beam is needed.

The base assumption in calibration is that the change of compressive force should be constant along the length of the member during the prestressing operation because the force is applied on both ends of the member with rigid steel blocks and the duct not yet grouted and therefore bond between tendon and beam does not exist.

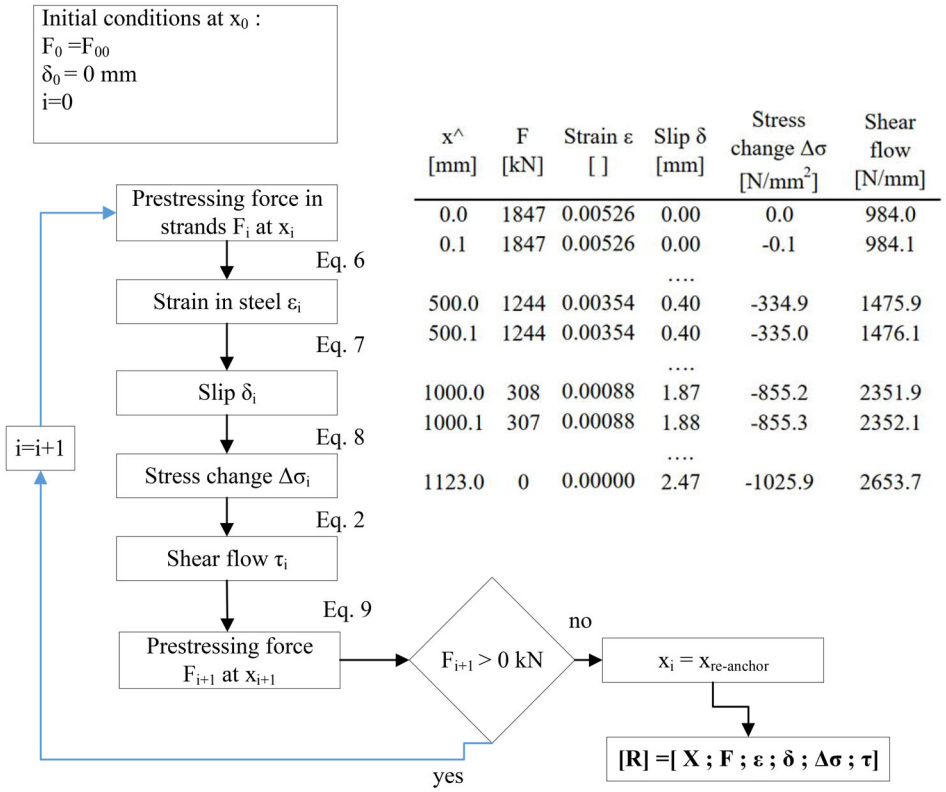

x^ [mm]	F [kN]	Strain ε [ ]	Slip δ [mm]	Stress change Δσ [N/mm²]	Shear flow [N/mm]
0.0	1847	0.00526	0.00	0.0	984.0
0.1	1847	0.00526	0.00	-0.1	984.1
			….		
500.0	1244	0.00354	0.40	-334.9	1475.9
500.1	1244	0.00354	0.40	-335.0	1476.1
			….		
1000.0	308	0.00088	1.87	-855.2	2351.9
1000.1	307	0.00088	1.88	-855.3	2352.1
			….		
1123.0	0	0.00000	2.47	-1025.9	2653.7

FIGURE 7 Numeric calculation procedure for re-anchoring length of broken tendon

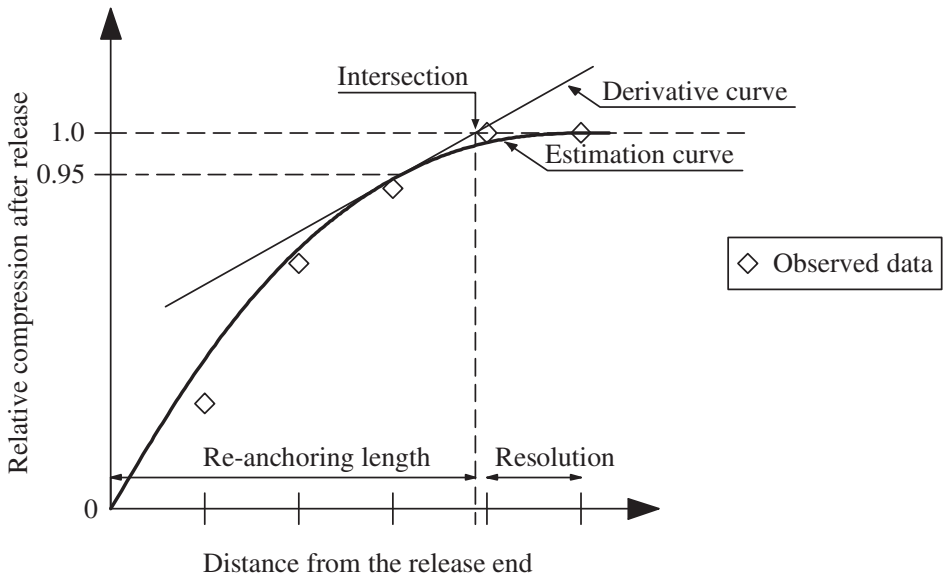

FIGURE 8 Principle of estimation of re-anchoring length

The strain gauges are calibrated by using the change of beam axial force due to anchorage loss at the end of beam prestressing. The value of force loss due the anchorage loss is relatively large (approximately 15–25% of the prestress force depending on the beam length) and the change is in the same direction as it is in the tendon re-anchoring tests. The calibration is based on the assumption that the change of normal force, normal stress and strain – due to anchorage take-up loss – should be constant along the beam length and in prestressing chairs during prestressing. During the calibration and in the test, the behavior of specimen is assumed linear elastic.

The method of analyzing the bond and re-anchoring length is based on fitting a third order polynomial curve on the test results that show the beam axial force along the beam length. This is done to find the location of the cross-section in which the change of strain equals zero during the test that is, all the force of released strand is transmitted to concrete with bond before the cross

TABLE 2 Compressive and tensile strengths of grout on test day

SET	Beam #	Compressive Strength μ / σ [MPa]	Tensile strength μ / σ [MPa]
I	1	34.0 / 1.2	3.0 / 0.7
	2	40.2 / 1.3	2.0 / 0.4
	3	35.8 / 1.8	2.0 / 0.6
	4	35.4 / 0.9	2.6 / 0.5
II	5	33.5 / 0.8	4.5 / 0.6
	6	35.2 / 1.8	4.7 / 0.6
	7	36.6 / 1.7	3.9 / 0.6
	8	30.9 / 0.9	4.5 / 0.3
III	9	31.8 / 1.1	6.3 / 0.8
	10	31.8 / 1.1	6.3 / 0.8
	11	34.2 / 1.4	5.0 / 0.9
	12	34.2 / 1.4	5.0 / 0.9
IV	13	34.7 / 1.1	4.5 / 0.4
	14	34.7 / 1.1	4.5 / 0.4
	15	28.4 / 0.4	4.0 / 0.6
	16	28.4 / 0.4	4.0 / 0.6

Abbreviations: μ, mean value ($n = 6$ for compressive, $n = 3$ for tensile strength). σ, standard deviation.

TABLE 3 Re-anchoring lengths of released tendons per release step and released force

		1st release Top strands		2nd release Middle strands		3rd release Bottom strands	
Test set	**Beam #**	**L_{REA} [m]**	**F_{REA} [kN]**	**L_{REA} [m]**	**F_{REA} [kN]**	**L_{REA} [m]**	**F_{REA} [kN]**
I set L = 3000 mm Complete grouting	1	1.01	574	1.18	1169[a]	1.25	1845
	2[b]	1.10	220[a]	1.24	403[a]	1.67	1580
	3	0.74	241[a]	0.81	592[a]	1.40	1564
	4	1.10	564	1.24	1119	1.53	1804
II set L = 3000 mm Incomplete grouting	5	1.83	595	2.04	1196	2.16	1792
	6[b]	2.18	567	2.37	1160	2.43	1725
	7	1.43	583	1.54	1153	2.13	1754
	8	1.79	575	2.04	1211	2.21	1874
III set L = 1230 mm Complete grouting	9	0.79	602	1.04	1234	1.26[e]	1847
	10	0.98	612	1.14	1186	1.34[e]	1797
	11	0.77	281[c]	0.93	850	1.21	1489
	12	0.81	560	0.95	1133	1.18	1711
IV set L = 1700 mm Incomplete grouting	13	1.99[e]	312[c]	N/A[d]	921	N/A[d]	1528
	14	1.41	593	N/A[d]	1203	N/A[d]	1823
	15	N/A[d]	612	N/A[d]	1232	N/A[d]	1867
	16	N/A[d]	597	N/A[d]	1226	N/A+	1835

[a]The release mechanism got stuck during the strand release and the strands did not release completely until the flame cutting in the last release.
[b]Unintentionally incomplete grouting suspected due to problems during grouting.
[c]Two strands released from the passive end before the start of the measurements.
[d]Released force did not re-anchor completely in the length of the beam.
[e]Re-anchoring was considered complete enough to allow for an estimation of the re-anchoring length beyond the beam length.

section. Without the curve fitting the determination of re-anchoring and bond length would be limited by strain gauge spacing. Due to bond characteristic, the estimation curve behaves with asymptotical manner towards the unity. The location of the point of intersection between the unity line of relative compression and the estimation curve is very sensitive to the parameters of the estimation. More stable results are achieved by setting the tangent curve on a selected point (0.95) of the estimation curve shown in Figure 8. The location of the intersection of the tangent curve and the unity of the relative compression is then solved.

4.2 | Re-anchoring test

In Tables 2 and 3 the re-anchoring forces and corresponding measured re-anchoring lengths are shown per strand release step and the relative compression stresses along the beam length after the last release are shown in Figures 9 and 10. The relative compression stress means the beam axial force relative to the prestressing force. The release of strands in different stages attempts to simulate gradual failure of the tendon from top to bottom. In almost all of the beams the re-anchoring length increases as more strands are released. It is also evident that the re-anchoring length is greatly increased if the grouting has a small void in the top of the duct.

When comparing long beams with complete grouting (I set) to short beams with complete grouting (III set), it can be seen that the re-anchoring length is larger in the long beams than in the short ones. One reason for this is that in short beams the released force did not completely re-anchor in the measurement range which affects the curve fitting method used to estimate the re-anchoring length. This is evident in Figure 10(a) where it can be seen that the relative compressive stress does not reach unity within the measurement range. It should be noted that the curves for long and short beams are quite similar in shape. Another reason for the difference in re-anchoring lengths may be the quality of grouting and grout, which is better in III set (see Table 2), even though the grout mixing properties were kept similar. This could be supported by the fact that the re-anchoring lengths show the same discrepancy even in the first release. In the IV set with short beams, the re-anchoring length cannot in most cases be determined since the released force could not be anchored in the beam length at all.

Since the complete re-anchoring length as single quantity does not give any information on the forces of the strands in the re-anchoring region, the intersection points of linearly interpolated re-anchoring data with 25%, 50% and 75% re-anchoring levels of released

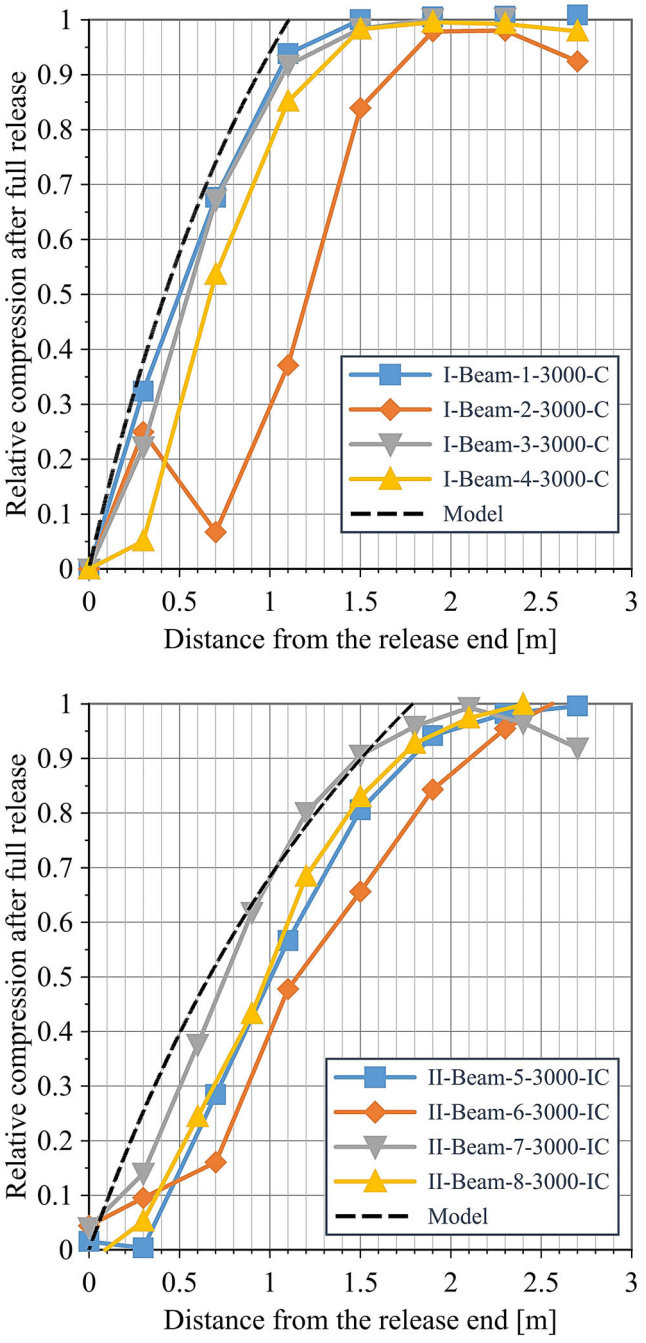

FIGURE 9 Relative compression in member cross sections in case of complete grout (left) and incomplete grout (right)

force is calculated. Calculation is done on each release step so that the re-anchoring properties for each released set of strands can be viewed individually. This allows also the determination of mean and 95% confidence interval values of re-anchoring lengths in said re-anchoring levels. The steps where the released force differed more than 100 kN from the intended value of 600 kN are ignored. This means that beams 2 and 3 are completely ignored here and first steps of beams 11 and 13 are also ignored. The results are shown in Figures 11, 12 and 13.

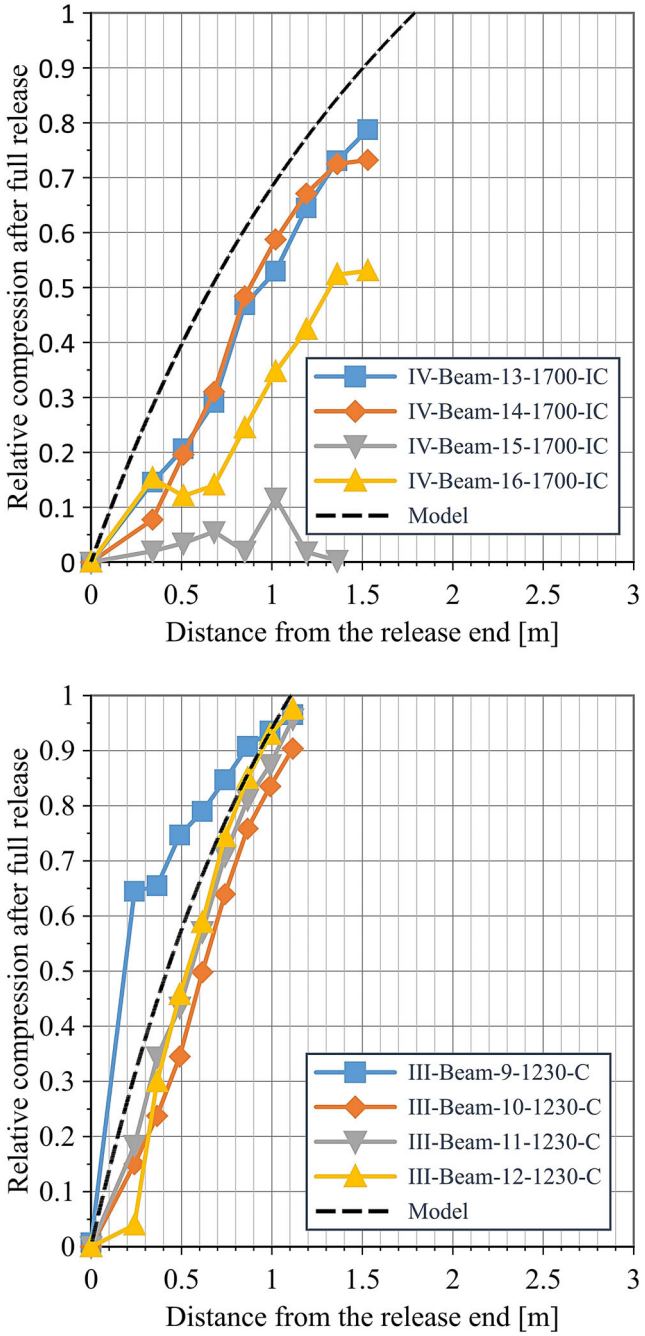

FIGURE 10 Relative compression in member cross sections in case of complete grout (left) and incomplete grout (right)

It is clear from the results that in incomplete grouting the re-anchoring length is higher in all force levels in comparison to complete grouting. The difference of re-anchoring length in complete and incomplete grout is smallest if only the four middlemost strands are considered. In the results of the topmost strands the difference of re-anchoring length between complete and incomplete grouting is highest. This is probably caused by the expansion of strand due to the releasing of force which causes grout spalling in void in case of incomplete grouting. Overall, the middlemost strands have the best re-anchoring capacity in this study.

It can be noted that in Figures 11-13 the deviation of the re-anchoring length remains almost constant despite the proportion of force being anchored. In all figures the distance between the mean curve and 95% CI curve remains almost constant. Deviation has only a slight increase when the proportion of re-anchored force increases in all cases.

It should be noted that in the tests the order of the strand release in the duct was from top to bottom, and therefore the released force also cumulates in accordance with the release phases, which could influence the results presented in Figures 11-13. The anchored force in the earlier release phases could affect the bond strength of the grout in the following releases because of the interaction between strands. That might explain the apparent increase in transfer length of the released force in all force levels in Figures 11-13. In case of incomplete grout, the anchoring length of the released force has a small decrease while the middle strands are released. The explanation of this is that the top strands re-anchor mostly on the grout below them (because there is a void above) and therefore interact with the middle strands, which have better re-anchoring conditions due to the surrounding grout. While the middle strands are released, the relative slip between the top and the middle strands is decreasing. This leads to the decrease of force in top strands.

4.3 | Pull-out tests

4.3.1 | Grout prism tests

Preliminary pull-out tests were executed to assess the magnitude of the bond length to determine the adequate length of the test beams. The grout prism tests were conducted by pulling strands from the grout prism. The strands were cast in grout prisms with no pretension to estimate the bond stress-slip relation, with the ultimate bond strength of tendon strand cast in grout neglecting the Hoyer effect. The bond length of strand in grout prism is 100 mm. The overall height of the prism is 200 mm and its area is 250 mm × 250 mm, Figure 14.

In these tests, the effect of adhesion (referring to the adhesion term in Equation (2) on bond stress is approximately 2 to 3 MPa. The variation of the value of adhesion is high which can be seen in Figure 14, in starting point of the curves with zero slip. In Equation 2, the adhesion term is a constant 3 MPa. In Equation (2) the term related to slip and the effect of lack-of-fit is 0.4. In Figure 14, there is deviation in the derivatives of curves and the corresponding slope of the slip and bond stress varies between 0.15 and 0.4. The

high variation in derivatives could be due to mixed effects of adhesion and slip-bond relation, or the different behavior of the loss of adhesion with high slip values in different test specimens. The ultimate bond stress also has high variation in cases of a single strand, with the ultimate bond stress varying between 3 MPa and 5.5 MPa with a slip value of 15 mm.

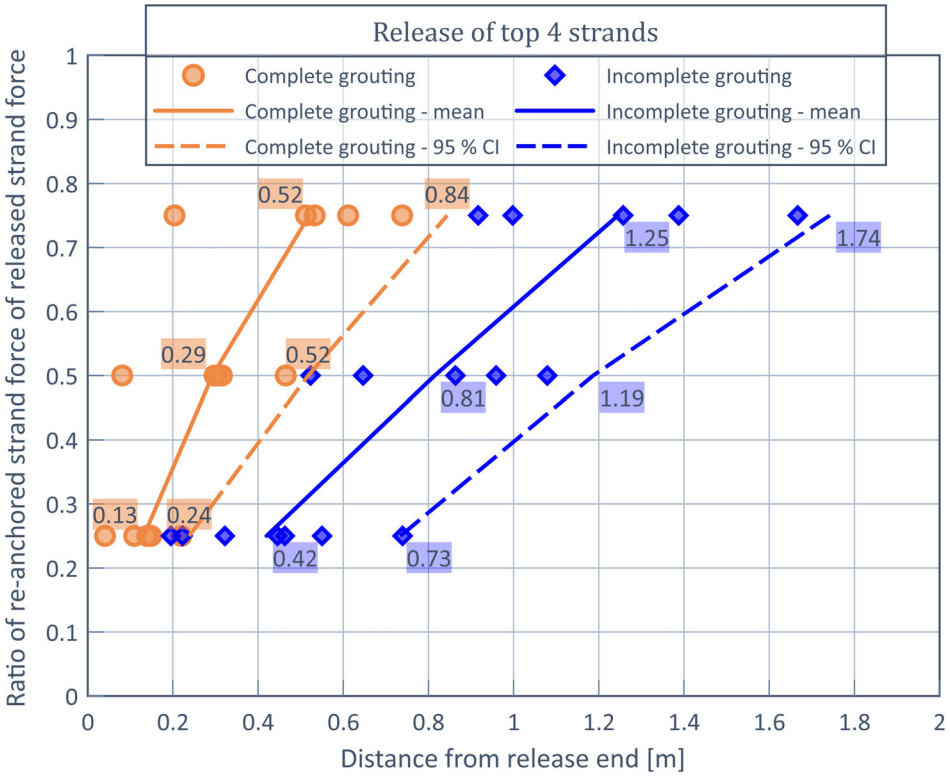

FIGURE 11 A re-anchoring length of released force levels of 25%, 50% and 75% in the release of top strands (#1...4)

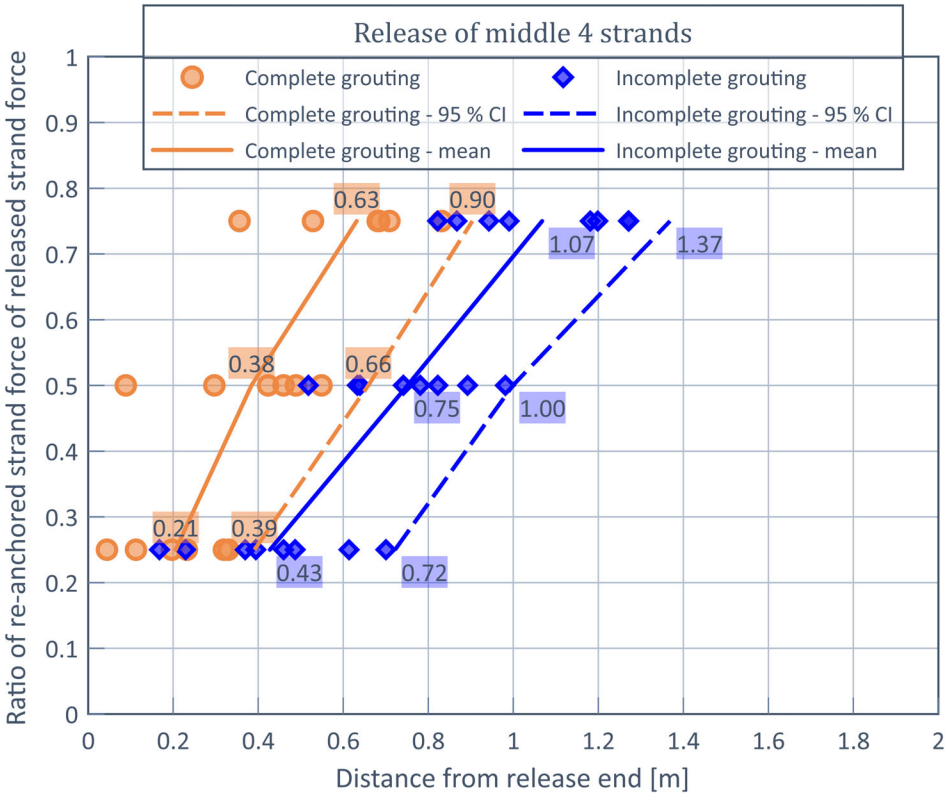

FIGURE 12 A re-anchoring length of released force levels of 25%, 50% and 75% in the release of middle strands (#5...8)

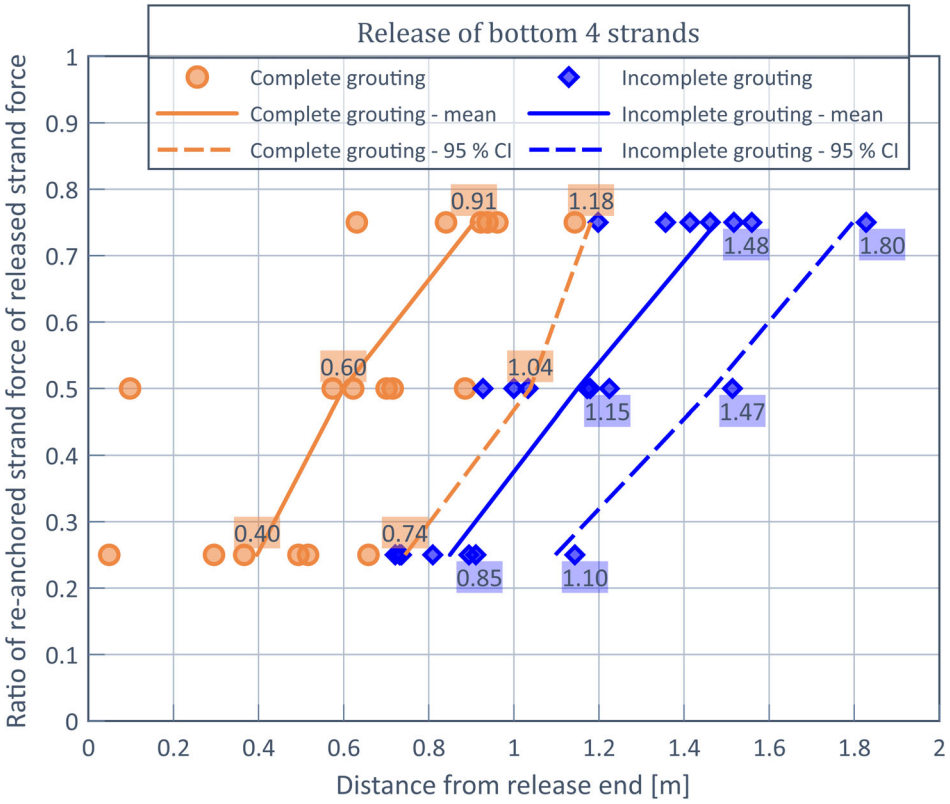

FIGURE 13 A re-anchoring length of released force levels of 25%, 50% and 75% in the release of bottom strands (#9...12)

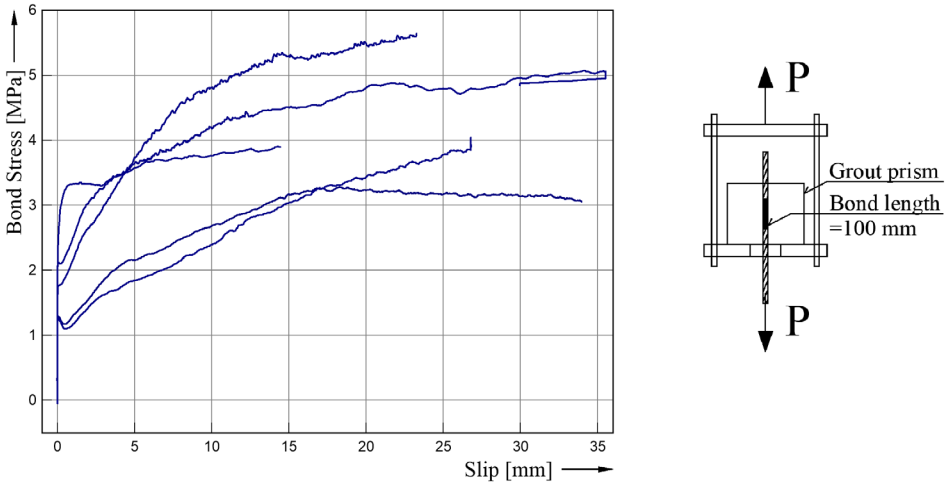

FIGURE 14 Single strand pull-out bond stress versus slip

4.4 | Tendon pull-out in the active end

The strands were pulled out during the test according to Figure 4 in the "test procedure" section. The bond length is assessed with a similar procedure as re-anchoring, which is described in previous section of this paper. The values of bond length (L_{TRA}) are collected in Table 4. The calculated drop at active end force is also tabulated. In Table 4, one can notice that the re-anchoring and bond are independent from each other in beam sets I and II, i.e. the length of the beam is long enough to develop re-anchoring in one end and a bond in another. The losses in the active end due to additional stressing and slip are only minor, resulting from local slip in the active end. In the final pull-out stage, the tendon slipped only in beam 6, in which an unintentional incomplete grouting is suspected.

In beam sets III and IV, these two phenomena overlaps, which means the beam is not long enough for the bond and re-anchoring lengths to develop separately. This leads to a permanent slip of the strands and loss of active end tendon force. In beam set III with complete grouting, the slip during additional stressing occurs in beams 9 and 10 after all of the

TABLE 4 Bond transfer lengths of tendons per pull-out step and release step

		1st pull-out Top strands released			2nd pull-out Middle strands released			3rd pull-out Bottom strands released			Final pull-out		
Test set	Beam #	L_{TRA} [m]	F_{PO} [kN]	ΔF_A [%]	L_{TRA} [m]	F_{PO} [kN]	ΔF_A [%]	L_{TRA} [m]	F_{PO} [kN]	ΔF_A [%]	L_{TRA} [m]	F_{PO} [kN]	ΔF_A [%]
I set	1	0.61	202	-1	0.58	220	-1	0.63	236	0	1.11	857	-4
L = 3000 mm	2[b]	0.51	202	-1	0.77	229	-1	-	-	-	1.13	1179	17[d]
Complete grouting	3	0.75	185	-2	-	-	-	1.07	238	1	1.33	1260	20[d]
	4	0.66	195	-2	0.69	235	-1	0.72	249	0	1.18	888	-2
II set	5	0.55	195	-2	0.60	236	-1	0.61	266	-0	1.44	964	2
L = 3000 mm	6[b]	0.86	265	-1	0.94	245	-0	1.24	294	-4	1.26	704	-27
Incomplete grouting	7	1.38	195	-1	1.23	213	-0	1.25	136	-0	2.11	758	9[d]
	8	0.59	176	-2	0.72	212	-11	0.59	224	0	1.54	825	-4
III set	9	0.38	198	-2	0.44	229	-2	0.82	269	-14	0.75	745	-92
L = 1230 mm	10	0.55	170	-1	0.51	189	-2	1.12	283	-16	1.00	777	-86
Complete grouting	11	0.44	183	-1	0.29	156	-2	0.49	217	-3	0.95	588	-95
	12	0.53	185	-1	0.44	205	-0	0.48	216	-2	0.90	813	-35
IV set	13	0.60	222	-21	N/A[a]	398	2	-	-	-	1.50	409	-78
L = 1700 mm	14	N/A[a]	137	-30	0.65	212	-1	0.64	252	-3	N/A[c]	525	-89
Incomplete grouting	15	N/A[a]	-33	-10	N/A[a]	189	-83	-	-	-	1.29	214	-27
	16	N/A[a]	170	-20	0.77	174	-14	1.09	168	-8	N/A[c]	412	-91

[a]Pull-out force could not be maintained in beam length, beam axial forces dropped below initial level.
[b]Unintentionally incomplete grouting suspected due to problems during grouting.
[c]Pull-out force did not transfer completely in the beam length, beam axial forces increased in beam length.
[d]Pull-out force transferred completely to the beam but strand movement in the active end caused the anchoring wedges to move and anchor the strands to a higher force.

strands are released from the passive end. During the final pull-out, the ultimate bond stress is reached and the force in the active end decreases almost to zero after the final pull-out.

In beam set IV the behavior of beams is more complex. In the first pull-out, there seem to be great slip which leads to a considerable loss of force in the active end after the first pull-out. In subsequent pull-out stages the loss of force in the active end is minor, with the exception of beam 15 in which a considerable loss occurred on the second pull-out stage. The explanation of the behavior of these beams is that the grout has spalled in the void and the ultimate bond is reached during the first pull-out after the top strands are released. In the second release and second pull-out the bond is better, because the middle strands are surrounded more completely by grout. Due to these reasons the force-slip behavior is ambiguous in beam set IV during pull-out, see notation 1) in Table 4. The evolution of re-anchoring and bond lengths in each release and pull-out step are shown in the annex.

4.5 | Calculation of bond length overlapping with re-anchoring length

The calculation of bond length in the beam in which the re-anchoring length of released strands overlaps the bond length is performed by applying the theory presented in Equations (6) to (9). A new term $\Delta\delta$ is added on the procedure

$$\Delta\delta_i = (\varepsilon_0 - \varepsilon_i) * \varsigma, \tag{10}$$

which means the change of slip on cross section i, due to pull-out force F_{P0}.

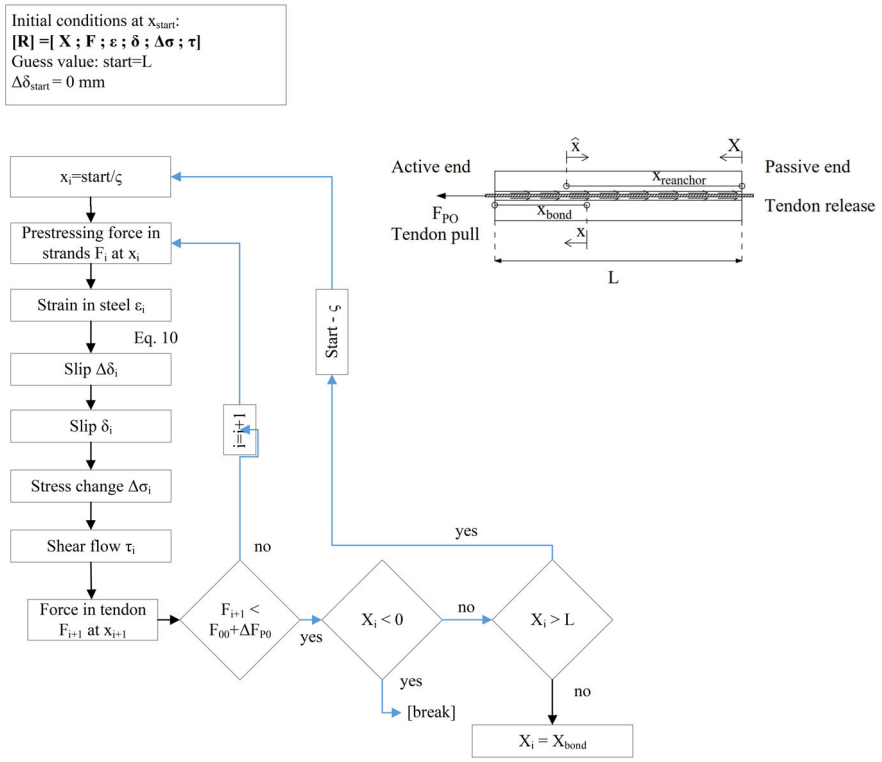

FIGURE 15 Numeric calculation procedure for actions in broken tendon exposed with pull-out force affecting on re-anchoring length. That is, overlapping re-anchoring and bond length

The calculation procedure for overlapping re-anchoring and bond length of the released strand bundle is presented in Figure 15. The initial conditions vector {R} of calculation are determined by the calculation process of re-anchoring presented in Figure 7. The determination of bond length is assessed with the same procedure as the length of re-anchoring. The aim of the process is to find out the cross section in which the pull-out force has zero effect. In that cross section the change of slip is $\Delta\delta = 0$ mm, due to the bond of the pull-out force. The process is calculated stepwise from cross section x towards the active end until the second condition is met, which means an equilibrium between bond stress and pull-out force is reached. If the cross section which satisfies the condition is outside of the beam, the location of the starting cross section is moved towards the passive end by ς and the iteration is started again.

In the case of overlapping re-anchoring and bond lengths the slip values increase significantly. In the case of the active end behaving independently, the order of the slip value with a 300 kN pull-out force is 0.13 mm. Whereas, in the case of the shorter beam with a lower distance between release and pull-out, the calculated value of slip is more than 3.5 mm with complete grout shown for test beam 9 in Figure 16(a) and 5.5 mm with incomplete grout in test beam shown in Figure 16(b).

The model presented in Equation (2) gives reasonable results when applied in cases in which re-anchoring and bond length are overlapping. According to preliminary pull-out tests with grout prism and single strand, the value of the ultimate bond stress should be in the order of 3..0.5 MPa. The calculation model 2 with no plastic range gives results that are a bit lower than that. In beam tests the highest observed shear flow between tendon and complete grout is in the order of 3 MN/m, which corresponds to the value of 9 MPa in bond stress calculated on the perimeter presented in Figure 5.

In Figure 17 the observed shear flow of released tendons shows a difference between complete and incomplete grouting. It seems that the confinement effect of grout and tendon duct has a significant effect on bond, Figure 17(a). With complete grouting the released tendon could develop high bond strength and shear flow, whereas in incomplete grouting the grout cover spalls towards the void, decreasing the bond strength and mobilized shear flow at the release end. The development of bond strength during pull-out shows that in case of complete grout the ability to develop a bond-related shear flow is higher also in cases of overlapping bond and re-anchoring lengths.

5 | CONCLUSION

In this paper it is shown that the broken strands in post-tensioned tendon can re-anchor in case of incomplete grout. The ability of strand re-anchoring has beneficial effect on robustness of the structure. The incomplete grout has an effect on the re-anchoring strength and re-anchoring length of the strands broken in the post-tensioned tendon. This can

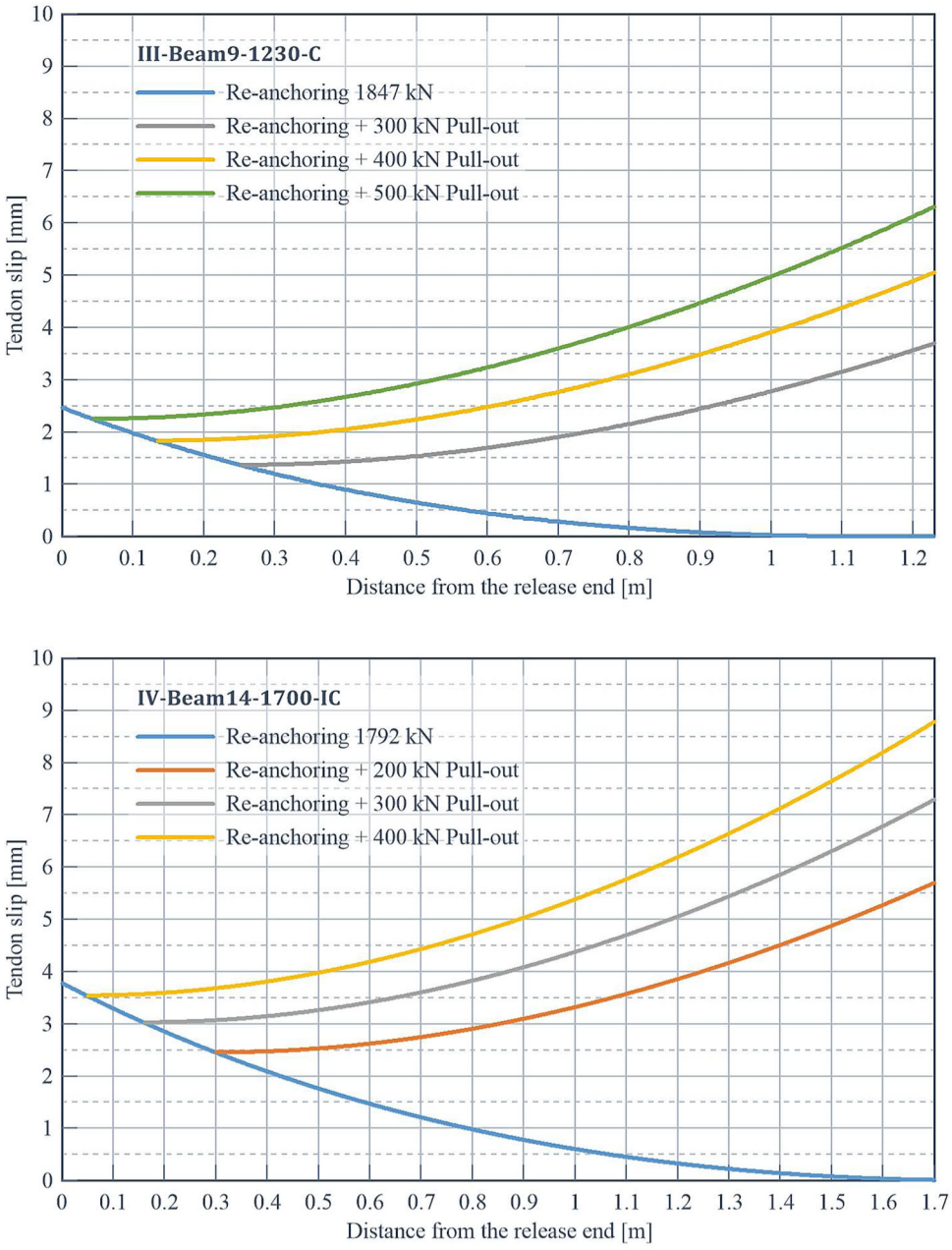

FIGURE 16 Strand slip according to model in Figure 15 with (a) grout L = 1230 mm (beam 9) (b) and (d) in-complete grout L = 1700 mm (beam 14)

be seen in all the strand locations; despite the fact that the void in grout is on the upper section of the duct, it still has an effect on strands located in the middle and at the bottom of the duct, with the release order progressing from top to bottom. The expansion of released strands in case of incomplete grouting cracks the grout towards the void and therefore the strength of the bond is decreased. In case of incomplete grouting the estimated re-anchoring length is 1.7 times in comparison to the re-anchoring length in complete grouting. It is noted that the anchoring length of the strands on top of the bundle is longer in comparison to other strands in the bundle.

The calculation of the re-anchoring length of the strand bundle in injection grout can be executed with the procedure presented in Reference 11. Despite the fact that the method is calibrated for single strands in concrete, the re-anchoring length shows a good match with the results of the tests, which are performed with a bundle of strands in injection grout. The reduction of bond and re-anchoring perimeter of bundle is shown to be an adequate method for calculation of respective lengths in case of incomplete grout. The results are also applicable for other tendon sizes (bundles of strands) by calculating the bond and re-anchoring perimeter for a strand bundle under consideration.

In longer (3 meters) test specimens, the bond and re-anchoring of the strands at the ends of the beam behave independently on each end of the beam, and these two phenomena do not overlap in beams with complete grout. The

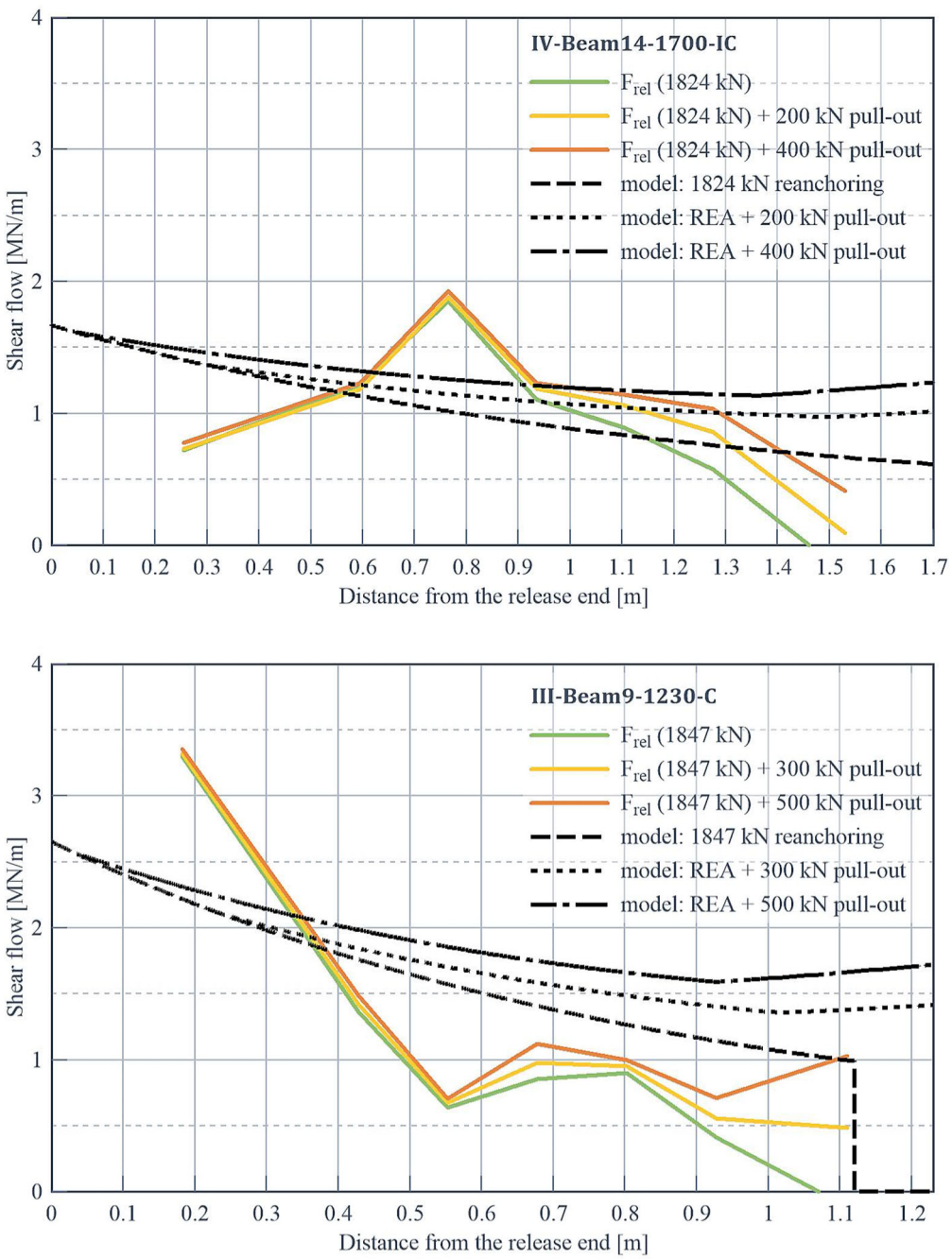

FIGURE 17 Shear flow distribution along the length of the beam (a) beam 9 with complete grout, (b) beam 14 with incomplete grout

independent behavior of the ends of the beam means that the breakage of tendon in real structures affects the structural behavior of the beam only locally, on a limited length. In shorter beams, (L = 1.2 and 1.7 meters) in which the re-anchoring and bond lengths overlap, the slip values increase significantly in comparison to longer specimens with the same pull-out force. This means that in real structures there might be uneven distribution of stresses between strands and between tendons in cases where stress increase is applied in the proximity of the strand breakage area and the bond length is overlapping with re-anchoring length.

The results are not only applicable to considerations of structures with bonded internal tendons, but also for many kind of structures with grouted tendons. There is a beneficial effect on robustness of grouted external tendon if the wire breakages occur in different cross sections with adequate re-anchoring distance between them. In this case the forces from broken wires can transfer to adjacent wires and the loss of wire has effect only on limited length. In case of unbonded strands or strands with long re-anchoring length, the overall loss of effective steel is the sum of losses of strand within the re-anchoring length.

FURTHER RESEARCH

Usually the corrosion deterioration of tendon strand wires is a slow process. And that is why the tendon force transfers from tendon to structure during long period of time. The creep characteristics of strand-grout interface in case of tendon failure should be assessed. What is the overall effect of creep on the re-anchoring or bond length.

The bond and re-anchoring behavior affects force distribution in the cross section. The uneven bond and slip behavior of strands leads to an uneven distribution of stresses in strands and tendons in the cross section. The robustness aspect of the beam cross section should be assessed. Also, the progressive failure of cross section strands with the zipper fashion of the beam should be considered.

ACKNOWLEDGMENTS

This research project was carried out at Tampere University, Department of Civil Engineering as part of the ETEVÄ Cooperation research program funded by the Finnish Transport Infrastructure Agency. Open access funding enabled and organized by Projekt DEAL.

DATA AVAILABILITY STATEMENT

Data available on request from the authors

ORCID

Olli Asp https://orcid.org/0000-0003-4022-8336

REFERENCES

1. Clark G. Post-tensioned structures–improved standards. Proc Ins Civil Eng Forensic Eng. 2013;166(4):171–9.
2. Wang L, Zhang X, Zhang J, Ma Y, Xiang Y, Liu Y. Effect of insufficient grouting and strand corrosion on flexural behavior of PC beams. Construct Build Mater. 2014;53:213–24.
3. Zhang L, Wang L, Zhang J, Liu Y. Corrosion-induced flexural behavior degradation of locally ungrouted post-tensioned concrete beams. Construct Build Mater. 2017;134:7–17.
4. Hansen B, Hansen B. Tendon failure raises questions about grout in posttensioned bridges. Civil Engineering. 2007;77(11):17–18.
5. Den Ujil JA. Bond and splitting action of prestressing strand. Int Conf Bond Concr Riga. 1992;15-17:2/79–88.
6. Balázs GL. Transfer control of Prestressing strands. PCI J. 1992; 37:60–71.
7. Martí-Vargas JR, Serna P, Navarro-Gregori J, Pallarés L. Bond of 13mm prestressing steel strands in pretensioned concrete members. Eng Struct. 2012;41:403–12.
8. EN-1992-1-1. Eurocode 2 Design of Concrete Structures: Part 1–1: General rules and rules for buildings.
9. Wang L. et al. Bond behavior between multi-strand tendons and surrounding grout: Interface equivalent modeling method. Constr Build Mater. 2019;226:61–71.
10. SFS-EN 523:2003. Steel strip sheaths for prestressing tendons. Terminology, requirements and quality control
11. FIB bulletin 10, 2000: Bond of reinforcement in concrete. State of the art report2000. 434.
12. SFS-EN 445:2007. Grout for prestressing tendons. Test methods. CEN 2007.

AUTHOR BIOGRAPHIES

Olli Asp, Tampere University, Faculty of Built Environment, Tampere, Finland.

Joonas Tulonen, Tampere University, Faculty of Built Environment, Tampere, Finland.

Lauri Kuusisto, Tampere University, Faculty of Built Environment, Tampere, Finland.

Anssi Laaksonen, Tampere University, Faculty of Built Environment, Tampere, Finland.

How to cite this article: Asp O, Tulonen J, Kuusisto L, Laaksonen A. Bond and re-anchoring tests of post-tensioned steel tendon in case of strand failure inside cement grouting with voids. *Structural Concrete*. 2021;1–18. https://doi.org/10.1002/suco.202000351